Pure & Appl. Chem., Vol. 62, No. 1, pp. 89–101, 1990.
Printed in Great Britain.

Role of high temperature chemistry in CVD processing

Karl E. Spear and Ryan R. Dirkx, Materials Science and Engineering,

The Pennsylvania State University, University Park, PA 16802

Abstract – High temperature chemistry principles are examined as important tools for developing an understanding of chemical vapor deposition (CVD) systems, and for predicting deposition behavior. An attempt is made to qualitatively predict the complex interdependencies among controllable experimental parameters, process variables, and deposition properties. Examples of silicon boride deposition from SiH_4, BCl_3, and H_2 mixtures are used to illustrate high temperature thermochemical modeling techniques which utilize the concept of local equilibrium.

INTRODUCTION

Chemical vapor deposition (CVD) has become an extremely important high temperature synthesis technique for coatings and powders. In a CVD process, gaseous species chemically react for form one or more condensed phase plus gaseous products. The chemistry involved in CVD is usually much more complex than in *physical vapor deposition* (PVD), a process in which gaseous species typically produced by evaporation or sputtering processes are condensed on a substrate. The present paper examines CVD processes, and particularly the *role of high temperature chemistry in CVD* as an aid in predicting the complex chemistry and deposition behavior as a function of experimentally controllable CVD parameters.

An excellent overview of *vapor deposition*, a term collectively used to include all CVD and PVD methods, and its many applications is given in a book edited by Bunshah (1). The development of specific deposition techniques for densifying composites and other porous bodies, *chemical vapor infiltration* (CVI), is reviewed by Naslain (2), and those for achieving *selective area or selective phase deposition* are reviewed by Carlsson (3). These and every commercial coating process have a goal of achieving a particular set of coating properties. These sets of prioritized properties drive the CVD development studies, the studies to determine the controllable parameters which will achieve the desired properties. For chemically complex systems, using trial and error methods to achieve these properties is too costly in terms of both money and time. This is why research to develop predictive CVD models is so important. The ability to predict coating properties from a knowledge of the controllable experimental parameters, and the influence of these parameters on process variables will typically impact a number of diverse applications for a particular coating.

Papers published over the past decade (refs. 4-9) have illustrated the value of high temperature thermochemical modeling techniques in CVD studies. The high temperature data needed for such modeling may be experimentally determined, or else predicted by calculational techniques and from established trends in high temperature behavior. More details on the uses of high temperature chemistry as a tool in developing an understanding of complex CVD processes is illustrated throughout this paper. The general areas of *high temperature chemistry*, and *modeling CVD processes* are described first. This is followed by an outline of the complex interrelationships that exist among experimental CVD parameters, process variables, and deposit properties. Finally, examples of silicon boride deposition (ref. 10) are presented to illustrate the value of thermochemical modeling in analyzing CVD behavior.

HIGH TEMPERATURE CHEMISTRY

High temperature chemistry has been defined by Leo Brewer as *the chemistry at temperatures which are high enough to cause significant differences from the expected room temperature chemistry.* (ref. 11) An effort to systematically understand the chemical behavior of materials at high temperatures was initiated by Brewer and co-workers more than forty years ago during the Manhattan Project. These studies resulted in the birth of high temperature chemistry as a major area of chemical research, one that involves the chemical, thermodynamic, kinetic, and structural properties of species, systems, and processes at high temperatures.

Generalizations about the chemistry of reactions and compounds at room temperature often do not hold as the temperature of a system is increased.(ref. 11) Chemical reactions which are not energetically favorable at room temperature may become important at high temperatures. Thermodynamic rather than kinetic limitations tend to determine high temperature reactivity. Vaporization processes and vapor species become increasingly important. Unusual compounds and vapor species which do not conform to the familiar oxidation states of the elements may form at high temperatures, and the complexity of the vapor phase increases. With increasing temperature, ordered

defect structures become disordered, and solid solution ranges increase significantly. Many of these effects result because reaction entropies gain in importance with respect to reaction enthalpies in determining the chemistry at high temperatures.

The above generalizations along with experiences in the laboratory led Searcy (12,13) to propose the first two "laws" of high temperature chemistry, and Margrave (14,15) to add a third. These are: *(i) at high temperatures, everything reacts with everything else, (ii) the higher the temperature, the more seriously everything reacts with everything else,* and *(iii) the products might be anything.* These laws humorously summarize the general essence of chemical trends in high temperature systems. Brewer (16-19) has shown that these laws are actually based on thermodynamic principles.

MODELING CVD PROCESSES

A CVD process involves gases flowing into a reactor where chemical reactions occur to produce a condensed phase plus gaseous products. These product gases plus unreacted or partially reacted input gases are then forced out of the reactor by the gas flow. A dynamic CVD process will achieve steady-state conditions unless fluctuations in temperature, total pressure, input gas composition, or flow rates or patterns dominate. The steady-state model plus local equilibrium concepts greatly simplify our ability to predict deposition behavior. Modeling deposition processes for a coating over a fixed geometric surface necessarily involves modeling not only the high temperature chemistry of the system, but also its mass transport and flow properties. This latter type of modeling has been reported for a few idealized systems with relatively "simple" chemistry (refs. 20-25), but the complexities of such chemically reactive flow models preclude their current use as a tool for most CVD studies.

The present discussions do not directly consider flow behavior and system geometry, but instead examine the *local high temperature chemistry* which can be predicted for a CVD system. The following discussion is intended to illustrate more clearly where our *local modeling* fits into a model for a complete CVD system.

Consider mentally placing a grid on a substrate to divide it into a finite number of cells which include the gas phase above the substrate. The present paper concerns the steady-state chemistry in each of these substrate cells, and the rates at which the mass transport and chemical processes occur within each cell. Coupling the residence time of the gas in each cell with the energy and mass transport from cell to cell would allow us to calculate the deposition behavior over an entire substrate. Of course, the system geometry and flow properties will determine the boundary conditions in each cell that are needed for calculating rates of deposition processes and the fraction of "input gas" that reacts within a given cell before transport to the next cell(s) occurs.

A simple physical model often used for describing a CVD system (refs. 5,6,9) is probably quite accurate for the substrate cell discussed above. As illustrated in Fig. 1, seven sequentially linked mechanistic steps describe the deposition process:

> The first and seventh steps are the respective forced flow of reactant gases into the system, and the forced exit of gases from the system.
>
> The second and six steps are the respective diffusion and bulk (viscous) flow of reactants from the bulk gas through a gaseous concentration boundary layer to the substrate, and the similar transport of product gases from the substrate out into the bulk gas.
>
> The third and fifth steps are the respective adsorption of gases onto the substrate, and desorption of adsorbed species from the substrate.
>
> The fourth step includes the deposition reaction as well as other chemical processes occurring on the surface.

High temperature research is needed for each of these steps, but is largely lacking for most CVD systems. For example, it is usually not known if the input gases react homogeneously before diffusing to the substrate surface, or if the rates of such reactions are slow in comparison to the transport rates. This information is required if we are to model the above second and third steps in the deposition process.

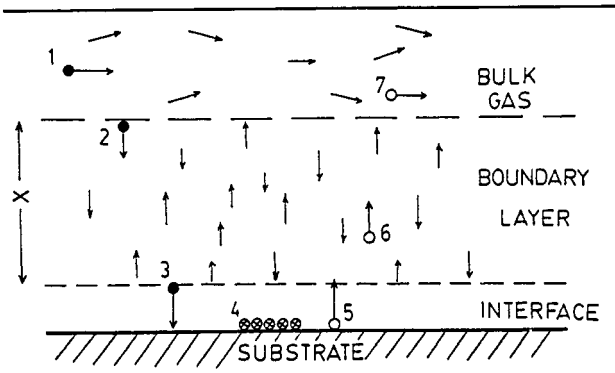

Fig. 1. Schematic Diagram Illustrating Seven Sequentially Linked Mechanistic Steps in a CVD Process.

The adsorption and desorption steps have typically not been studied for the species and substrate or coating surfaces of interest. However, it is sometimes possible to deduce from experimental deposition results whether the desorption of important species such as HCl(g) could be rate-limiting, or if an abundant species like hydrogen is preferentially occupying (poisoning) the surface sites.

The fourth step, the surface reactions, may be a complex set of chemical reactions. The chemistry of the adsorbed species, relative species concentrations and activities, collision frequencies, lifetimes of adsorbed species, surface diffusion rates, reaction rates, and thermodynamic limits on the reactions are all examples of useful high temperature chemistry information for CVD modeling studies.

COMPLEXITIES OF CVD PROCESSES

The interrelationships in a CVD system among controllable experimental **parameters**, process **variables**, and coating **properties** are extremely complex, which means modeling a CVD system is extremely complex. This section summarizes a first attempt to qualitatively define these interrelationships to provide a framework for organizing experimental observations, and for deducing experimental parameter changes which would lead to desirable coating properties. A more thorough discussion of these complex interrelationships has been given by Dirkx (10).

Generic listings are given in Table 1 for experimentally controllable parameters, process variables in a thermally activated CVD reactor, and typical coating properties of interest. These lists could of course be modified for a specific system being used to produce a coating with specific properties.

TABLE 1. Listings of the Interrelated Experimentally Controllable Process Parameters, the Process Variables, and the Coating Properties.

Controllable Experimental **Parameters**	Process **Variables**	Coating **Properties**
1. Reactor Geometry	1. Gas Temperature	1. Morphology
2. Substrate Temperature	2. Flow Behavior	2. Composition
3. Substrate Environment	3. Mean Gas Velocity	3. Thickness
4. Input Gas Composition	4. Gas Chemistry	4. Density
5. Total Flow Rate	5. Gas Homogeneity	5. Uniformity
6. Total Pressure	6. Deposition Rate	6. Adhesion
7. Substrate Surface	7. Deposition Surface	7. Crystallinity
8. Time of Deposition	8. Nucleation Density	8. Stress
9. Experimental Procedure		

The importance of understanding the relationships among these parameters, variables, and properties is illustrated by the simple schematic diagram shown in Fig. 2. Experimental parameters can be varied based on operator experience and "trial and error" methods until a coating with desired properties is achieved. Alternatively, models for the deposition system can be used to calculate the controllable parameters needed to achieve the desired deposition results. For complex chemical systems, the modeling techniques are needed to at least limit the parameter space most likely to yield the optimum deposition conditions.

Fig. 2. Schematic Relationship Among Experimental Parameters, Process Variables, and Coating Properties.

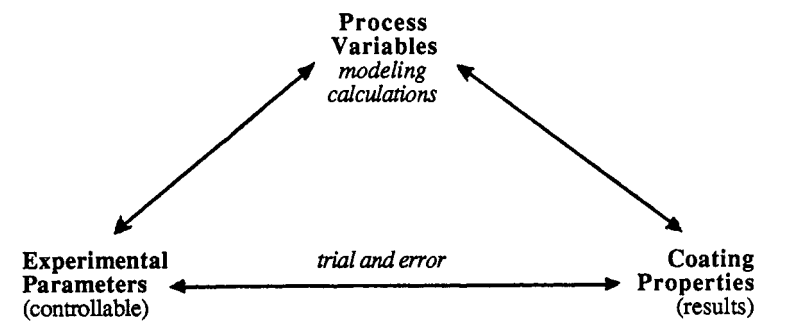

Modeling requires understanding the influence of experimental parameters on process variables, and the influence of process variables on coating properties. Our attempts to qualitatively predict the interdependencies are shown in Tables 2 and 3.

TABLE 2. Experimental **Parameters** Influence on Process **Variables.** The "x" qualitatively indicates a measurable dependence.

Experimental	Influence on Process **Variables** *							
Parameters	1 GT	2 FB	3 MGV	4 GC	5 GH	6 DR	7 DS	8 ND
1. Reactor Geometry	x	x	x	x	x	x	x	x
2. Substrate Surface	-	x	-	-	-	x	x	x
3. Substrate Temperature	x	x	x	x	x	x	x	x
4. Substrate Environment	x	x	-	x	x	x	x	-
5. Input Gas Composition	x	x	-	x	x	x	x	-
6. Total Flow Rate	x	x	x	x	x	x	x	-
7. Total Pressure	x	x	x	x	x	x	x	-
8. Time of Deposition	-	x	-	-	-	-	x	-
9. Experimental Procedure	-	-	-	-	-	-	x	x

* Process **Variables** are represented by the following numbers and the variable initials:
1. Gas Temperature; 2. Flow Behavior; 3. Mean Gas Velocity; 4. Gas Chemistry;
5. Gas Homogeneity; 6. Deposition Rate; 7. Deposition Surface; 8. Nucleation Density

TABLE 3. Process **Variables** Influence on Coating **Properties.** The "x" qualitatively indicates a measurable dependence, the "S" a strong dependence.

Process	Influence on Coating **Properties** *							
Variable	1 Mor	2 Com	3 Thi	4 Den	5 Uni	6 Adh	7 Cry	8 Str
1. Gas Temperature	x	S	-	x	x	-	x	-
2. Flow Behavior	x	x	x	-	S	-	-	-
3. Mean Gas Velocity	x	x	-	-	x	-	-	-
4. Gas Chemistry	x	S	x	x	x	x	-	-
5. Gas Homogeneity	x	S	-	-	S	x	-	-
6. Deposition Rate	x	-	S	x	S	-	S	S
7. Deposition Surface	S	x	-	x	S	S	x	S
8. Nucleation Density	x	-	-	S	S	S	x	-

* Coating **Properties** are represented by the following numbers: 1. Morphology;
2. Composition; 3. Thickness; 4. Density; 5. Uniformity; 6. Adhesion; 7. Crystallinity;
8. Stress.

The information in Tables 2 and 3 could be misleading in that the actual interrelationships are more complex than indicated. Many of the process variables are dependent upon other process variables. For example, the experimental parameter of substrate temperature influences the process variable of gas temperature, which influences the flow behavior, the gas chemistry, and thus the deposition rate. The flow behavior influences transport processes, and thus deposition rate. The substrate temperature directly influences the surface reaction rates, and thus deposition rate.

In spite of the complexities of the CVD parameter-variable-property interrelationships, extremely useful modeling can be performed. The complex interrelationships can often be qualitatively determined, and can sometimes be quantitatively calculated. Quantitative limits on deposition behavior can often be predicted, as can the sensitivity of deposition to changes in experimental parameters. A knowledge of the high temperature chemistry and energetics of the chemical system is critical for all of these CVD process predictions.

PREDICTING CVD BEHAVIOUR USING THERMOCHEMICAL MODELING

Equilibrium calculations provide a powerful tool for gaining insight into both equilibrium and non-equilibrium vapor deposition processes. Thermochemical modeling can be used to predict deposition behavior and to explain experimental observations such as:

(i) condensed phases which will deposit at equilibrium,
(ii) maximum rates or efficiencies of deposition,
(iii) partial pressures of all gaseous species in homogeneous equilibrium before any condensed phases are deposited,
(iv) partial pressures of all gaseous species in heterogeneous equilibrium with the condensed deposit,
(v) sensitivity of the above predictions to changes in experimentally controllable parameters, and
(vi) mechanistic possibilities for explaining non-equilibrium behavior.

Examples of thermochemical modeling results for the Si-B-H-Cl system are used to illustrate the above types of predictions of limiting deposition behavior and molecular mechanisms responsible for the deposition. Both theoretical and experimental results on the deposition of silicon borides from precursor gases of SiH_4, BCl_3, and H_2 are discussed (ref. 10). However, before presenting these examples, the critical concept of local equilibrium must be discussed.

(a) Local equilibrium – a critical concept for thermochemical modeling

Many people question the value of thermochemical modeling of CVD systems since *equilibrium* calculations are being used, and CVD is clearly a dynamic, *non-equilibrium* process. The reason thermochemical modeling is so useful as a tool in predicting and explaining CVD behavior is that *local equilibrium* will always be achieved by a portion of the chemical processes in a CVD system. That portion of the overall system can then be analyzed using equilibrium thermodynamic calculations. Such results often provide limiting values for deposition parameters for a system. For example, at temperatures high enough for mass transport of gaseous species through a concentration boundary layer to and/or from the substrate to be rate limiting (steps 2 and/or 6 in Fig. 1), the chemical reactions at the substrate surface are in *local equilibrium* (step 4 in Fig. 1). Calculations of the surface equilibrium indicate which species are important in the deposition processes, and provide partial pressures (activities) which are needed to calculate diffusion to and from the substrate. The extent of the changes in the equilibrium results with changing experimental parameters can also provide insight into the sensitivity of the deposition behavior to these experimental parameters.

It is not uncommon for the experimental composition of gas at the equilibrium surface to be different from that calculated by allowing the bulk input gas to reach heterogeneous equilibrium at the surface. This difference between the gas compositions for the experimental surface and calculated equilibrium surface depends on a number of factors, including two primary ones of: (i) the difference in the ratio of elements in the deposited phase and in the bulk input gas, and (ii) the difference in mass transport efficiencies of the elements to and from the surface (a variety of species may contribute significantly to the transport of a particular element). This topic has been discussed in more detail previously (ref. 6). In spite of these differences between the bulk gas composition and that of the gas arriving at the surface to cause deposition, the surface reactions still attain equilibrium at high temperatures, and equilibrium calculations can provide a method for deducing these compositional differences. Reasonable changes in the input gas for the surface equilibrium calculations can be made until the calculated results agree with the experimental observations. The changes necessary to achieve this "forced agreement" between the experimental and modeling results can provide insight into mechanisms for a deposition process.

An example for this valuable use of thermochemical modeling (and local equilibrium) is for the case in which the rate-limiting step for deposition is either the adsorption or desorption of a particular gaseous species at the substrate. We considered such a case in the deposition of Nb_3Ge in the Nb-Ge-H-Cl system (ref. 26). If the product gas HCl removal from the surface is rate limited by desorption, then its concentration will build up at the surface, and equilibrium calculations of deposition behavior must include increased quantities of HCl in the input to the calculations. Comparisons of modeling results with experimental observations can in general provide insight into the nature and extent of kinetic barriers to deposition.

(b) Auxiliary data and procedures for the Si–B–H–Cl deposition modeling

The auxiliary high temperature chemistry data required for the above such predictive calculations must be published, measured, or predicted through correlations or calculations in order to perform even the simplest modeling studies. Thus, the vital role of high temperature chemistry is again apparent. Thermodynamic modeling calculations requires a knowledge of the chemical compositions and solid solution ranges of **all** possible gaseous species and condensed phases which can exist in the temperature and system composition ranges of interest. For our CVD calculations on the Si-B-H-Cl system, thirty-three gaseous species and five solid phases (no solid solutions) were used.

The required thermodynamic stabilities as a function of temperature for most of the gaseous species were available in the JANAF Tables (27). We developed a self-consistent set of data for the five solid phases in the Si-B system using free energy - phase diagram relationships (ref. 28). Each individual calculation required specifying the concentrations (relative flow rates) of starting components, and the equilibrium temperature and total pressure. Typical conditions chosen for both the calculations and the experimental studies were:

Temperature	1000 - 1800K
Total Pressure	0.0263 atm (2,665 Pa)
BCl_3 flow rate	30 sccm *
SiH_4 flow rate	10 sccm
H_2 flow rate	1000 sccm

* sccm = standard cubic centimeters per minute

Each calculation represents one point on the diagrams given below. The computer program used in the present study was a slightly modified version of SOLGASMIX written by Eriksson (29-31).

(c) CVD phase diagrams

Generating CVD phase diagrams for a deposition system is one of the first types of thermodynamic modeling calculations that should be performed. These diagrams map the experimental parameters that will produce *equilibrium deposition* of a phase or phases of interest. Fig. 3 is an example of a *deposition temperature* versus *input gas composition* CVD diagram for the Si-B-H-Cl system. The temperature range is from 1300 to 1800K, while the input gas composition in terms of a ratio of [B/(B+Si)] ranges from 0.5 to 1.0 in this diagram. The diagram is for a constant total pressure of 0.0263 atm., and a constant $[H_2/(BCl_3+SiH_4)]$ of 25.

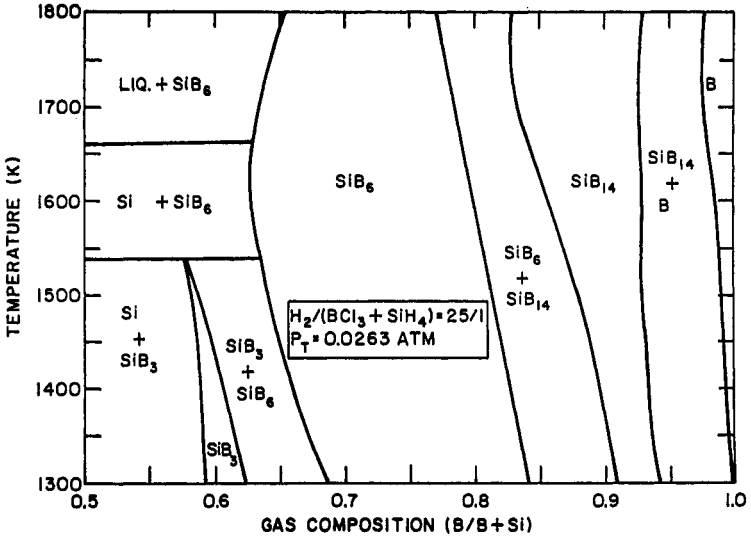

Fig. 3. CVD Phase Diagram for Input Gases SiH_4-BCl_3-H_2. The gas composition axis refers to the input gases, and the temperature to the deposition temperature. The diagram predicts which condensed phase(s) deposit at equilibrium under the given experimental conditions.

These CVD phase diagrams provide a broad overview of the experimental parameter space in which the desired phase or phases can be deposited. The CVD diagram in Fig. 3 shows that small changes in experimental parameters will cause the system to shift from the single phase SiB_3 deposition region. The deposition of single phase SiB_3 may be experimentally difficult, and quite sensitive to fluctuations in experimental parameters. The CVD diagram also shows that the temperature - composition range which will produce SiB_6 at equilibrium is large. However, possible deviations between calculated and experimental deposition may be expected for both SiB_3 and SiB_6 since the ratio of the elements in these condensed phases is significantly different from the ratio of these elements in the input gas required to deposit these phases. The diagram indicates that the surface gas composition will probably be richer in silicon than the bulk input gas composition.

The effects of doubling the hydrogen concentration on a portion of the above temperature versus composition CVD phase diagram is illustrated by Fig. 4. This figure shows the segment of the diagram in Fig. 3 which contains the single phase SiB_3 region, but at two different hydrogen concentrations. The phase boundaries for single phase deposition are shifted considerably by hydrogen. Fig. 5 shows the effect of changing hydrogen concentration by replacing the [B/(B+Si)] axis on the diagram in Fig. 4 with a changing $[H_2/(BCl_3+SiH_4)]$ ratio. This diagram shows that the addition of more hydrogen to the reactant gas favors the deposition of more silicon-rich phases. These diagrams in Figs. 4 and 5 depicting the effects of hydrogen on the deposition of SiB_3 could also be combined into a three dimensional representation, showing the combined effects of changing two compositional parameters and temperature.

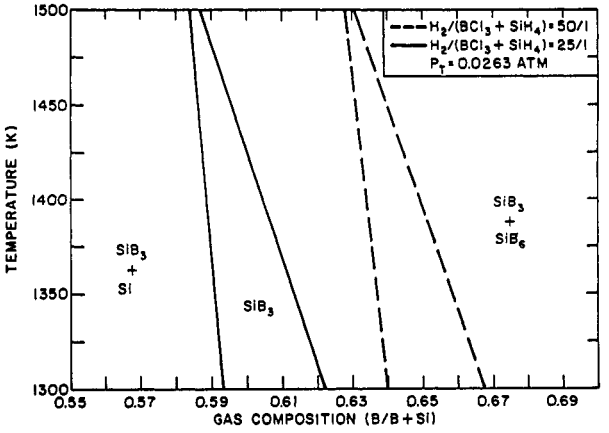

Fig. 4. CVD Phase Diagram Illustrating the Effect of Doubling the H_2 Concentration on the Single Phase Triboride Region.

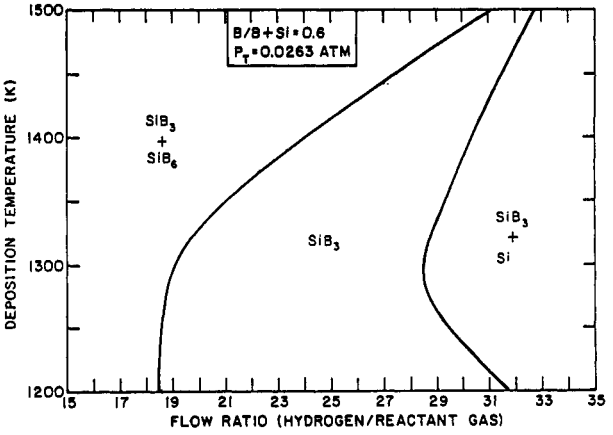

Fig. 5. CVD Phase Diagram Illustrating the Effect on the Single Phase Triboride Region of Changing the Input H_2 Concentration while Maintaining a Constant Input [B/(B+Si)] Ratio.

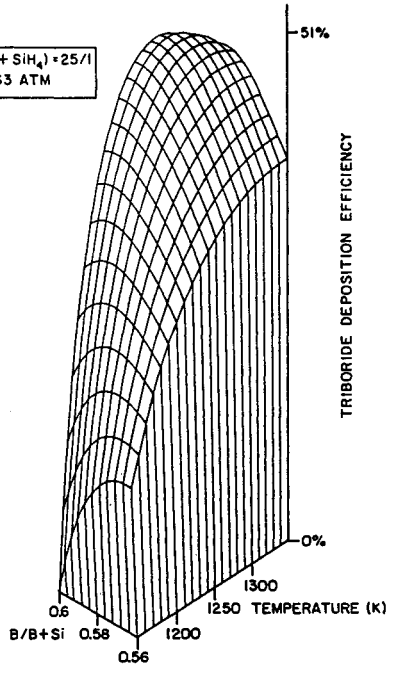

Fig. 6. Triboride Deposition Efficiency Surface as a Function of Input Gas Composition and Deposition Temperature. Efficiency is defined as the equilibrium deposition rate divided by the rate if no kinetic or thermodynamic barriers to deposition existed.

In Fig. 6, a temperature versus composition diagram which contains the single phase SiB_3 region is extended into the third dimension by an efficiency axis for the deposition of SiB_3. (Efficiency is defined as the equilibrium deposition rate divided by the rate if no kinetic or thermodynamic barriers existed.) This figure clearly shows that uniform deposition rates are not expected if the gas composition or temperature changes over the surface on which SiB_3 is deposited.

At 1150K in Fig. 6, the SiB_3 deposition efficiency is practically zero at an [B/(B+Si)] ratio of 0.60, but then increases as this ratio decreases to 0.56. An explanation for this behavior is related to the stabilities of the chloride gaseous species. As the [B/(B+Si)] ratio increases, so does the chlorine content of the gas since its only source is BCl_3. The higher the concentration of chlorine in the bulk gas, the higher the fractions of silicon and boron that remain in the gas phase rather than depositing as solid SiB_3.

Also shown by Fig. 6 is that the efficiency of SiB_3 deposition increases rapidly with increasing temperature. As temperature is increased, the hydrogen reduction of the chlorides is more favorable, and thus the deposition of solid SiB_3 increases. The rationalization of the results plotted in Fig. 6 are enhanced by considerations of partial pressure data presented in the next section.

(d) Limits on gas phase chemistry

CVD phase diagrams depict the condensed phases which can deposit at equilibrium for various sets of experimental parameters, but no information is given about which gaseous species may play important mechanistic roles in the deposition process. Detailed in situ gas phase diagnostics could provide the critical information, but these are difficult measurements that are not likely to be performed routinely on CVD reactors.

Modeling studies can provide predictive guidelines on important gaseous species in a CVD process, especially for high temperature operating conditions under which mass transport to and/or from the growing surface is rate limiting. Gas diffusion to and from the deposition surface (steps 2 and 6 in Fig. 1) is driven by partial pressure gradients across the concentration boundary layer between the surface and the bulk gas. For mass transport limited deposition, the surface gases achieve equilibrium with the deposited solid. As a first approximation for the gas partial pressures (activities) at this surface, equilibrium values can be calculated for the input gas composition at the total pressure and temperature of the deposition process. Deviations from this approximation will be discussed later in the next section.

Two limiting values for the partial pressures in the bulk gas may be approximated. The first is that the input gas species do not react until reaching the deposition surface, and that the product species are quickly swept out of the system. This approximation dictates that for diffusion calculations, all partial pressures in the bulk gas are zero except for the input species, whose partial pressures are calculated from their input mole fractions and the total system pressure.

The second approximation for the bulk gas partial pressures is that homogeneous equilibrium is reached in the input gas phase without the formation of a condensed phase. Whether or not the gas phase reaches homogeneous equilibrium depends not only on the basic kinetic properties of a chemical system, but also on the reactor design and operating conditions; for example, a hot-wall versus cold-wall reactor, the gas residence time in the reactor (flow rates, reactor dimensions), the gas collision frequency (total pressure, temperature).

Figs. 7a and 7b show the respective partial pressures of silicon and boron containing gaseous species calculated as a function of temperature for homogeneous gas phase equilibria (no solid phases were allowed to form). These figures also show the input gas partial pressures for the case in which no chemical reactions occur in the bulk gas. The experimental parameters utilized in these calculations were: total pressure (0.0263 atm), BCl_3 (30 sccm), SiH_4 (10 sccm), and H_2 (1000 sccm). Figs. 8a and 8b show the results of similar calculations for the deposition surface when the gas has equilibrated with SiB_3(s), the phase experimentally deposited under these conditions.

In the limiting case of no reactions of the input species, the silicon and boron are transported to the deposition surface as SiH_4 and BCl_3, respectively. The equilibrium partial pressures at the deposition surface given in Figs. 8a and 8b show that the silane partial pressure is below the limit of this graph, and the boron trichloride partial pressure, although initially high at low temperatures, quickly decreases with increasing temperature.

In the limiting case of homogeneous equilibrium in the bulk gas, Fig. 7a shows that $SiCl_2$ is the most abundant silicon containing species at temperatures greater than 1000K, while $SiCl_3H$ is the most abundant at lower temperatures. At the equilibrium deposition surface, the $SiCl_4$ partial pressure depicted in Fig. 8a is relatively large at temperatures of about 1000K and lower, but then quickly drops off. Above 1200K, the dominant silicon containing species at the surface is $SiCl_2$, but its partial pressure is more than an order of magnitude smaller than in the homogeneously equilibrated bulk gas.

If the input gases homogeneously equilibrate and the deposition is limited by mass transport processes (the deposition reactions reach equilibrium), the results in Figs. 7a and 8a predict the dominating net diffusion of silicon from the bulk gas to the surface occurs by $SiCl_3H$ at the lower temperatures, and by $SiCl_2$ at the higher temperatures. At lower temperatures, a significant net diffusion of $SiCl_4$ in the opposite direction from the surface to the bulk gas is predicted. As the temperature increases, this latter outward net diffusion rapidly decreases because of decreasing partial pressures of $SiCl_4$ in the system. This conclusion helps to explain the low deposition efficiency of SiB_3 at low temperatures which was indicated previously by the efficiency diagram in Fig. 6.

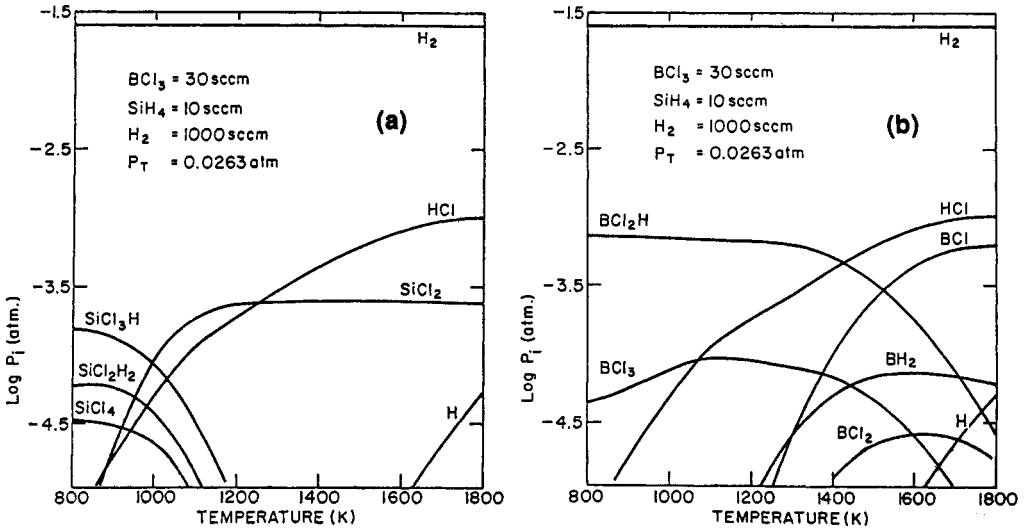

Fig. 7. Temperature Profiles of the Partial Pressures of the Predominant Gaseous Species in Homogeneous Equilibrium (no condensed phases are allowed): (a) Silicon-Containing Species, (b) Boron-Containing Species. If the input gases did not react, they would have the following partial pressures [in $\log_{10}$(atm)]: SiH_4 (-3.60), BCl_3 (-3.12), H_2 (-1.58).

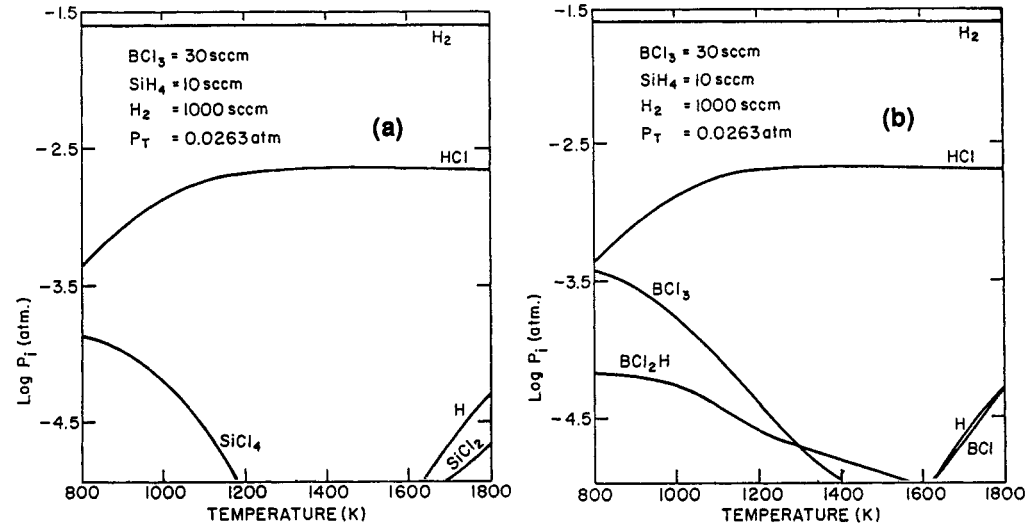

Fig. 8. Temperature Profiles of the Partial Pressures of the Predominant Silicon Containing Gaseous Species in Heterogeneous Equilibrium with Deposited SiB_3: (a) Silicon-Containing Species, (b) Boron-Containing Species.

Fig. 7b shows that BCl_2H is the dominant boron containing gas up to about 1500K in a homogeneously equilibrated bulk gas. Above this temperature, BCl dominates. At the equilibrium deposition surface, Fig. 8b shows the BCl_3 partial pressure to be dominating for boron containing species at the deposition surface for temperatures up to about 1200K, then BCl_2H and finally BCl take over, although the partial pressures of these latter species are always small in the temperature range depicted.

If the input gases homogeneously equilibrate at lower temperatures, the results in Figs. 7b and 8b predict the net diffusion of BCl_2H from the bulk gas to the surface, and a net diffusion of BCl_3 in the opposite direction from the surface to the bulk gas. As the temperature increases, this latter outward net diffusion decreases because the BCl_3 partial pressure decreases. Eventually the net direction of BCl_3 diffusion reverses because this species partial pressure decreases more rapidly at the surface than in the bulk gas with increasing temperature.

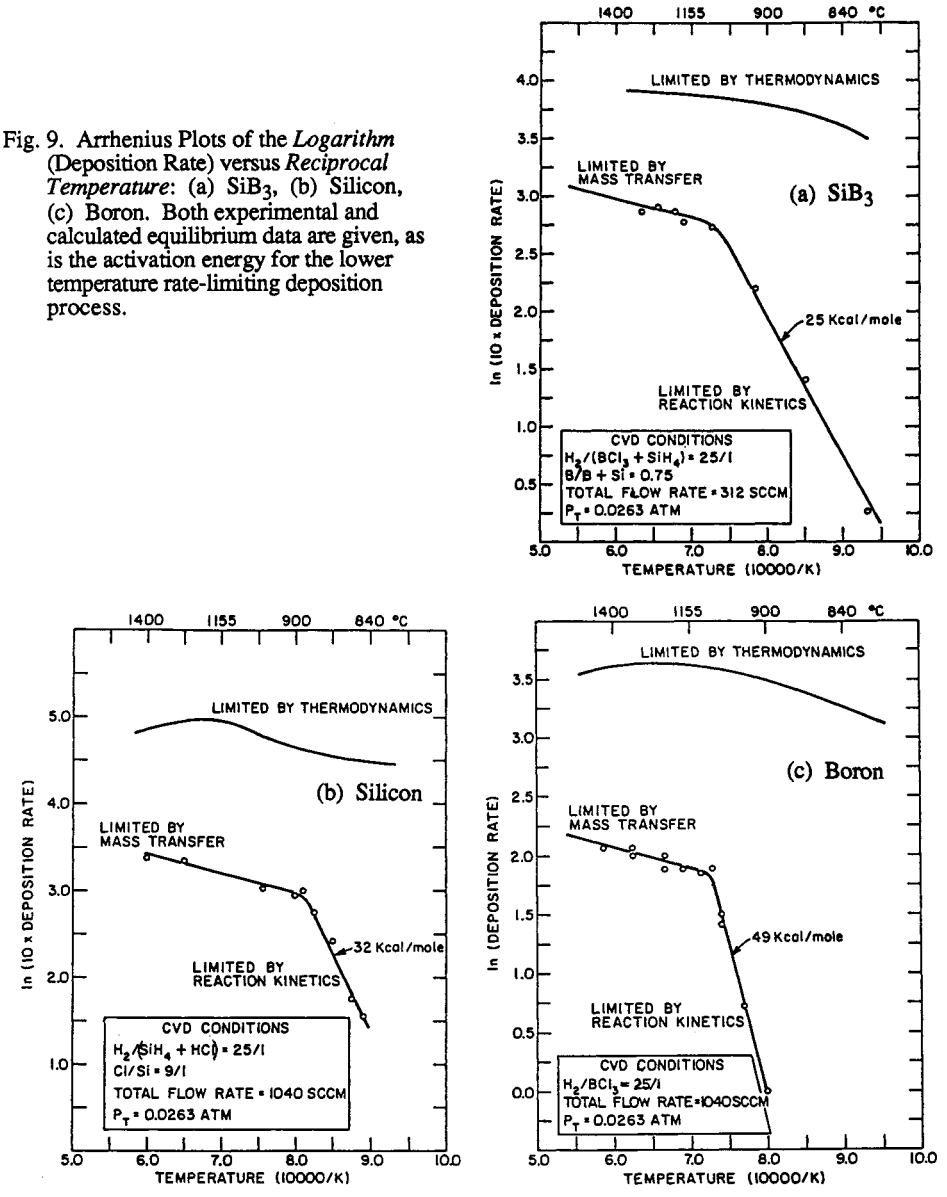

Fig. 9. Arrhenius Plots of the *Logarithm* (Deposition Rate) versus *Reciprocal Temperature*: (a) SiB_3, (b) Silicon, (c) Boron. Both experimental and calculated equilibrium data are given, as is the activation energy for the lower temperature rate-limiting deposition process.

(e) Deviations from predicted deposition behaviour

Thermochemical modeling utilizes equilibrium calculations, but much can be learned about nonequilibrium behavior and other deviations from predicted "equilibrium behavior" through the use of local equilibrium concepts. The following examples illustrate such analyses.

Deposition studies as a function of temperature for input gas compositions of $[B/(B+Si)] = 0.75$ and $[H_2/(BCl_3+SiH_4)] = 25$ and a total pressure of 0.0263 atm produced SiB_3 at 1100 to 1500K even though the CVD phase diagram calculations depicted in Fig. 3 predicted the formation of SiB_6. The first thought may be that the CVD phase diagram is not accurate because of uncertain system chemistry (for example, not including important gaseous species in the calculations) or because of uncertain thermodynamic data. The sensitivity of the CVD diagram to these uncertainties was considered, and such explanations for the differences between observed and calculated behavior were ruled out.

Two additional explanations resulted from analyses making use of thermochemical modeling. One partial explanation involves the deposition kinetics, the change from reaction kinetics limiting the deposition at lower temperatures to mass transport limiting the deposition rate at higher temperatures. The second explanation involves differences between the overall steady-state composition of the gas at the deposition surface and the bulk gas.

(i) Deposition rate limiting processes

Experimental rate investigations and equilibrium rate calculations were performed for the deposition of the three solids SiB_3, Si, and B (ref. 10), and the data were analyzed in terms of the Arrhenius plots [logarithm (deposition rates) versus 1/T] shown in Figs. 9a, 9b, and 9c. Attempts were made to simulate the SiB_3 deposition conditions when performing the Si and B studies. For example, HCl was added to the SiH_4 and H_2 input gases in the Si deposition studies since chlorine appears to react with silicon in the SiB_3 deposition. The conditions experienced by the elements in the triboride deposition experiments, however, are not identical to those in the elemental deposition studies, so the following analysis does not compare the absolute rate data from these figures.

The slopes in each of the above figures for the experimental high temperature rate data are similar to those for the calculated equilibrium data. This is expected at high temperatures when mass transport through a gaseous concentration boundary layer is rate limiting (ref. 6). The relatively large difference between experimental and equilibrium rates in this high temperature range is at least partially explained by the fact that a cold-wall reactor was used in the experimental studies (ref. 10).

The low temperature data are characterized by slopes related to activation energies for each rate limiting chemical reaction. The break between the low and high temperature slopes occurs at about 1400K for the SiB_3 and B deposition, but around 1150K for the Si deposition. These data are consistent with a mechanism for SiB_3 deposition in which the Si and B deposit "independently" and then react to form the triboride. For such a mechanism, equilibrium at the SiB_3 deposition surface cannot occur until the temperature is high enough for equilibrium to be achieved in both the Si and B deposition processes; this is what is experimentally observed.

At temperatures from about 1150K and higher, the Si deposition reactions reach equilibrium at the substrate, while the B deposition processes are limited by reaction kinetics below 1400K. At temperatures above 1400K, the reactions should reach equilibrium for the deposition of SiB_3, Si, and B, and all three deposition systems should be limited by mass transport of gaseous species.

As was discussed at the beginning of this section, the CVD phase diagram in Fig. 3 predicts the equilibrium deposition of SiB_6 for the experimental parameters used, yet SiB_3 was observed ar 1100 - 1500K. The above rate data could explain this difference at low temperatures when the deposition of boron, but not silicon, was limited by reaction kinetics. However, above 1400K, no chemical kinetic limitations are expected, so the observed deposition of SiB_3 at higher temperatures must be rationalized in other ways. This is done in the following paragraphs.

(ii) Steady-state surface concentrations

The observed high temperature deposition of SiB_3, when equilibrium calculations and the above kinetic analysis predicted SiB_6 deposition, is analyzed below in terms of the steady-state chemistry at the deposition surface.

The experimentally used input gas composition of [B/(B+Si)] = 0.75 is rapidly depleted in boron if SiB_6 is deposited since the [B/(B+Si)] ratio is 0.86 in this solid. Comparisons of calculated gas phase chemistry in equilibrium with SiB_6 at 1500K with that in equilibrium with SiB_3 showed a major difference to be that the SiB_6 containing system contained ten times more $SiCl_2$ at equilibrium. What this means in terms of the deposition process is that if SiB_6 begins to form during the initial stages of deposition, as predicted by the CVD phase diagram in Fig. 3, $SiCl_2$ will begin to concentrate at the deposition surface. This would occur as long as SiB_6 is being deposited until a steady-state is reached in which the $SiCl_2$ rate of formation at the surface is equal to its rate of removal from the surface by mass transport through the gaseous boundary layer into the bulk gas stream.

The effects of a buildup of $SiCl_2$ at the deposition surface can be predicted using thermochemical modeling, as is illustrated by Fig. 10. This figure is a CVD phase diagram at a constant temperature of 1500K, with the horizontal axis representing the input gas composition of SiH_4 and BCl_3 by the ratio [B/(B+Si)]. The vertical axis is a measure of the excess $SiCl_2$ buildup at the deposition surface by a ratio of the excess $SiCl_2$ moles over the total input gas moles. A value of 1.0 on that axis corresponds to 10.4 moles of excess $SiCl_2$ over the 10 moles of SiH_4 and 30 moles of BCl_3 and 1000 moles of H_2 metered into the system at a composition of 0.75 for [B/(B+Si)].

At a value of 0.0 on the vertical axis in Fig. 10, which represents the behavior of the initial reactant gas before any dichloride buildup occurs, and at a [B/(B+Si)] input gas ratio of 0.75, the equilibrium deposition of SiB_6 is clearly predicted. Moving up the vertical axis at a constant [B/(B+Si)] input gas ratio of 0.75 shows that the buildup of $SiCl_2$ at the surface will eventually cause the deposition to shift from SiB_6 to SiB_3. This would occur at a ratio of about 25:10 for $SiCl_2$(excess):SiH_4(input), quite a large number. However, it is seen that such a large ratio is not necessary if the effect of the excess dichloride on the horizontal [B/(B+Si)] axis is taken into account. At an input gas composition of 0.75 for [B/(B+Si)], and a value of 0.5 on the vertical excess axis, the total ($SiCl_2$ + SiH_4) moles is 15, while the total BCl_3 moles is 30. This excess $SiCl_2$ causes a shift in the [B/(B+Si)] ratio from 0.75 to 0.67, which along with being at 0.5 on the vertical axis is almost enough to move into the single phase SiB_3 region of Fig. 10. Thus, instead of needing a ratio of 25:10 for $SiCl_2$(excess):SiH_4(input) at the surface to cause the equilibrium deposition of single phase SiB_3, a ratio of just over 5:10 is needed.

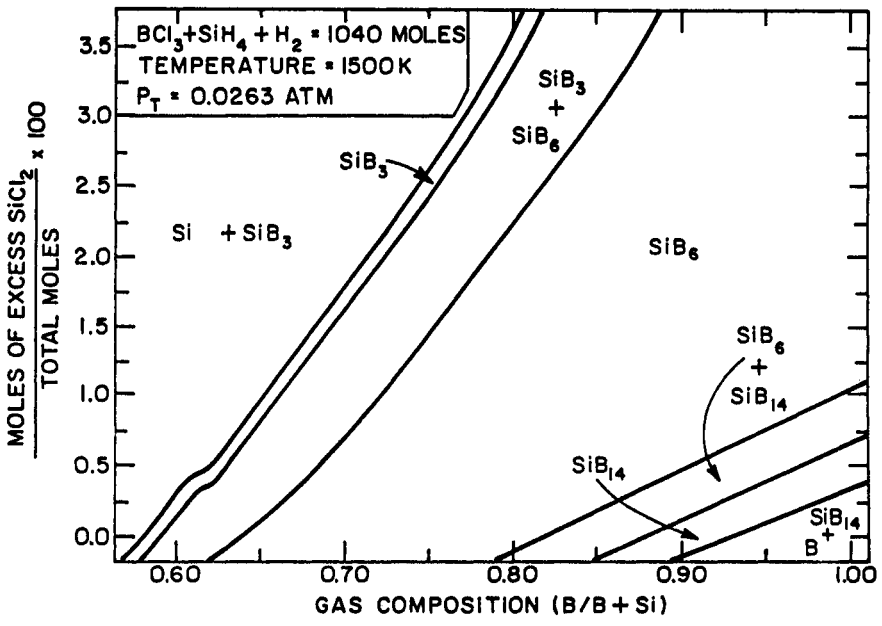

Fig. 10. CVD Phase Diagram at a Constant 1500 K Illustrating the Effect of an Excess Concentration of $SiCl_2$ at the Deposition Surface. The input H_2 is 1000 moles, while the sum of the BCl_3 and SiH_4 input is 40 moles. Thus, every unit on the vertical axis represents 10.4 moles of excess $SiCl_2$ in addition to the input precursor gases.

Calculations similar to those described above for the buildup of excess $SiCl_2$ at the deposition surface were performed to determine the possible influence of HCl, the major product gas in the deposition reactions. The results showed that a buildup of HCl at the surface would cause a shift from SiB_6 deposition toward more boron rich phases, the opposite of what was experimentally observed. However, a depletion of HCl at the surface from the equilibrium amount would cause a shift in deposition behavior toward SiB_3. The fast removal of HCl from the deposition surface was discounted as a possible explanation for the observed deposition of SiB_3 on the basis of experiments from Mehalso and Diefendorf (32). They studied the deposition of boron by the hydrogen reduction of BCl_3, and concluded on the basis of kinetic results that the rate limiting process for the deposition was the slow removal of HCl from the deposition surface.

SUMMARY

The discussed complex interdependencies among controllable experimental parameters, process variables, and deposition properties in a CVD system could easily discourage any attempts to develop an understanding of such systems. In spite of these complexities, many valuable analyses and predictions of deposition behavior can be made using the principles of high temperature chemistry, particularly high temperature thermochemistry. Many times the resulting predictions of deposition behavior are only numerically approximate or qualitative in nature, but they can still dramatically limit the range of conditions for deposition, or correctly give the trends in deposition behavior with changing experimental parameters.

Extremely efficient CVD research can be performed through a combination of a solid experimental program that is closely coupled with modeling studies. The combination of the two types of research yields much more than the sum of the two individual efforts, and either one by itself is of limited value if complex chemical systems are being examined. The value of this close coupling was illustrated by the high temperature thermochemical modeling that was used in explaining the experimental silicon boride deposition behavior. Making use of local equilibrium concepts in setting up thermochemical modeling calculations for explaining experimental observations in a dynamic CVD system is critical. This is true for modeling any dynamic chemical process, whether it involves CVD, vaporization, corrosion, or reactions at interfaces in composite systems. The logic for understanding and modeling each of these systems is quite similar.

Acknowledgements

The CVD investigations reported in this paper were largely supported by the Ceramics Program, Division of Materials Research, U.S. National Science Foundation.

REFERENCES

1. R.F. Bunshah, ed., Deposition Technologies for Films and Coatings, Noyes Publications, Park Ridge, NJ (1982).
2. R. Naslain and F. Langlais, High Temperature Science, Proc. 6th International Conference on High Temperatures: Chemistry of Inorganic Materials, National Institute of Standards and Technology, Gaithersburg, MD, April 3-7, 1989. (in press)
3. J.O. Carlsson, High Temperature Science, Proc. 6th International Conference on High Temperatures: Chemistry of Inorganic Materials, National Institute of Standards and Technology, Gaithersburg, MD, April 3-7, 1989. (in press)
4. K.E. Spear, Proc. 7th International Conference on Chemical Vapor Deposition (CVD-VII) [T.O. Sedgwick and H. Lydtin, eds.] The Electrochemical Society, Pennington, NJ (1979), pp. 1-16.
5. K.E. Spear, Pure & Appl. Chem. 54(7), 1297-1311 (1982).
6. K.E. Spear, Proc. 9th International Conference on Chemical Vapor Deposition (CVD-IX) [McD. Robinson, C.H.J. van den Breckel, G.W. Cullen, and J.M. Blocher, and P. Rai-Choudhury, eds.] The Electrochemical Society, Pennington, NJ (1984), pp. 81-97.
7. C. Bernard, High Temperature Science, Proc. 6th International Conference on High Temperatures: Chemistry of Inorganic Materials, National Institute of Standards and Technology, Gaithersburg, MD, April 3-7, 1989. (in press)
8. C. Bernard, Proc. 8th International Conference on Chemical Vapor Deposition (CVD-VIII) [J.M. Blocher, G. Vuillard, and G. Wahl, eds.] The Electrochemical Society, Pennington, NJ (1981), pp. 3-16.
9. T.M. Besmann, Surface Modifications Technologies [T.S. Sudarshan and D.G. Bhat, eds.] The Metallurgical Society, Warrendale, PA (1988), pp. 311-325.
10. R.R. Dirkx, Phase Behavior in the Silicon-Boron System: Preparation of Silicon Borides by Chemical Vapor Deposition, Ph.D. Thesis in Solid State Science, The Pennsylvania State University (1986).
11. K.E. Spear, Treatise on Solid State Chemistry, Vol. 4 [N.B. Hannay, ed.] Plenun Press, New York (1976), pp. 115-192.
12. A.W. Searcy, International Symposium on High Temperature Technology, McGraw Hill, New York (1960), p. 336
13. A.W. Searcy, Chemical and Mechanical Behavior of Inorganic Materials [A.W. Searcy, D.V. Ragone, and U. Colombo, eds.] Wiley, New York (1970), pp. 15-32.
14. J.L. Margrave, High Temperature Materials and Technology [I.E. Campbell and E.M. Sherwood, eds.] Wiley, New York (1967), pp. 21-55.
15. J.L. Margrave and G. Mamantov, High Temperature Materials and Technology [I.E. Campbell and E.M. Sherwood, eds.] Wiley, New York (1967), pp. 78-127.
16. L. Brewer, Inorganic Chemistry (Section of 16th Int. Congr. of Pure and Applied Chemistry, Paris) Butterworths, London (1958), pp. 559-570.
17. L. Brewer, The Chemistry and Metallurgy of Miscellaneous Materials: Thermodynamics [L.L. Quill, ed.] McGraw Hill, New York (1950), pp. 193-275.
18. L. Brewer, Topics in Modern Inorganic Chemistry [W.O. Milligan, ed.] Robert A. Welch Foundation, Houston, TX (1963), pp. 47-92.
19. L. Brewer, J. Chem. Educa. 35, 153-156 (1958).
20. M.E. Coltrin, R.J. Kee, and J.A. Miller, J. Electrochem. Soc. 131, 425-434 (1984).
21. M.E. Coltrin, R.J. Kee, and J.A. Miller, J. Electrochem. Soc. 133, 1206-1213 (1986).
22. K.F. Jensen, Proc. 9th International Conference on Chemical Vapor Deposition (CVD-IX) [McD. Robinson, C.H.J. van den Breckel, G.W. Cullen, and J.M. Blocher, and P. Rai-Choudhury, eds.] The Electrochemical Society, Pennington, NJ (1984), pp. 3-17.
23. D.E. Rosner, R. Nagarajan, S.A. Gokoglu, and M. Kori, Proc. 10th International Conference on Chemical Vapor Deposition (CVD-X) [G.W. Cullen and J.M. Blocher, eds.] The Electrochemical Society, Pennington, NJ (1987), pp. 61-80.
24. P. Tsui, Theoretical and Experimental Studies of Convective Effects on Chemical Vapor Deposition, Ph.D. Thesis in Ceramic Science, The Pennsylvania State University (1988).
25. F. Rosenberger, Proc. 10th International Conference on Chemical Vapor Deposition (CVD-X) [G.W. Cullen and J.M. Blocher, eds.] The Electrochemical Society, Pennington, NJ (1987), pp. 11-22.
26. C.F. Wan and K.E. Spear, Calphad 7(2), 149-155 (1983).
27. M.W. Chase, C.A. Davies, J.R. Downey, D.J. Frurip, R.A. McDonald, and A.N. Syverud, JANAF Thermochemical Tables, 3rd Edition, American Insitute of Physics, New York, NY (1986); also J. Phys. Chem. Ref. Data 14 (Suppl. 1) (1985).
28. R.R. Dirkx and K.E. Spear, Calphad 11(2), 147-155 (1987).
29. G. Eriksson, Acta Chem. Scand. 25, 2561-2568 (1971).
30. G. Eriksson and E. Rosen, Chemica Scripta 4, 193-194 (1973).
31. G. Eriksson, Chemica Scripta 8, 100-103 (1975).
32. R.M. Mehalso and R.J. Diefendorf, Proc. 5th International Conference on Chemical Vapor Deposition (CVD-V) [J.M. Blocher, H.E. Hintermann, and L.H. Hall, eds.] The Electrochemical Society, Pennington, NJ (1975), pp. 84-98.